INFLUENCE OF AIR FLOW ON BLISK VIBRATION BEHAVIOUR

B. Beirow, A. Kühhorn, S. Schrape
Brandenburg University of Technology, Chair of Structural Mechanics and Vehicle Vibration Technology
Siemens-Halske-Ring 14, D-03048 Cottbus
Germany

OVERVIEW

Based on a simple mechanical model of a high pressure compressor (HPC)-Testblisk called equivalent blisk model (EBM) the influence of the air flow on the forced response is studied in principle. In the first step the EBM has to be derived based on a finite element analysis of the disk from design and an adjustment of experimentally determined blade alone frequencies in order to consider blade mistuning. Applying the EBM – so far not considering the air flow influence – to carry out forced response analyses due to a rotating excitation acting on the stationary blisk, a maximum blade displacement amplification of more than 50 % has been calculated comparing the tuned and the mistuned blisk. Aiming at an additional consideration of the air flow, fully coupled computations of the fluid structure interaction (FSI) are exemplarily carried out for elastically supported blades in a cascade arrangement. The results are used to calibrate simple mass-spring-damper models from which additional aerodynamic elements considering the co-vibrating air mass, air stiffening or aerodynamic damping can be derived. This information is applied to extend the EBM to a so called advanced EBM. Results of forced response calculations, now including aerodynamic influences, show that for an extreme application to a rear blisk close to the combustion chamber a strong smoothing of originally localised vibration modes occurs. The maximum blade displacement amplification due to mistuning is partly decreased from more than 50 % to below 7 % for the first blade flap mode.

1. MOTIVATION

Initiated from the requirement for an effective reduction of fuel consumption and simultaneous power enhancement of future aero engines more and more light weight solutions have been realised in the last years. Among these the **bl**ade integrated d**isk** (blisk) technology integrated in high pressure compressors (HPC) has become significant (FIG 1). However, since manifold mechanisms of aerodynamic excitation remain, a number of particularities affecting the vibration behaviour such as low mechanical damping compared to separate blade-disk constructions, mistuning and mode localisation phenomena are connected to this kind of design. Especially mode localisations are associated with high stress and strain levels in the blades and thus will negatively affect the fatigue strength. Additional influences result from fluid-structure interactions which could affect blade vibrations in a damping or exciting manner. In order to guarantee a save and predictable operation on the one hand and further enhancements of the design on the other hand, a more improved understanding of the complex structural dynamical behaviour of blisks as well as the specific fluid-structure interactions (FSI) becomes necessary.

Since critical mode localisation phenomena primarily result from blade mistuning [13], it is purposeful to identify mistuning distributions experimentally by means of so called blade alone frequencies. A corresponding approach for weakly coupled blisks as also dealt with in the present paper is demonstrated and applied in [1]. Based on the experimental results and supported by results of a finite element analysis, an equivalent blisk model (EBM) composed of lumped masses, spring and damper elements is derived, firstly without a consideration of effects resulting from FSI. Apart from the main purpose of the model, which is to carry out forced response calculations with regard to the relevant engine orders, it is additionally suited to correct mean shifts of experimentally determined mistuning distributions resulting from blade-disk-couplings in an iterative way. In order to study the influence of the air flow on the structural forced vibration response in principle, additional aerodynamic elements are included in the model. The basic choice of aerodynamic elements orientates to results of a fully coupled FSI analysis of a simplified compressor cascade configuration via the coupling tool MpCCI [14]. Additional parameter studies regarding the aerodynamic elements show that the fluid structure interaction essentially affect vibration modes. Especially strong localisations in original modes are attenuated.

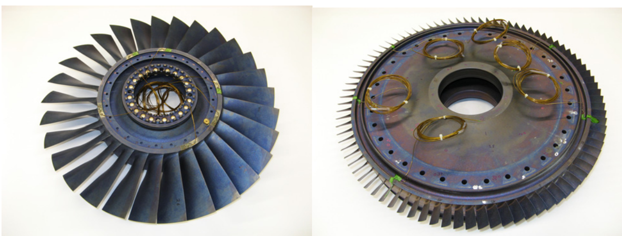

FIG 1. HPC-Test-Blisks of E3E-Phase I Program

2. EXPERIMENTAL IDENTIFICATION OF MISTUNING

Since blade mistuning is directly reflected in the distribution of blade-alone-frequencies, it suggests itself to identify it within the scope of an experimental blade frequency determination. Thus, numerical models could be up-dated regarding the consideration of mistuning. A suitable procedure of mistuning identification is based on ‘blade by blade’-measurements applying a step by step impact excitation of each blade and a simultaneous acquisition of vibration velocity response data from a laser vibrometer. In order to produce repeatable impacts, a device keeping and moving the miniature hammer is applied (FIG. 2). In this way, frequency response functions (FRF) of all blades could be derived which are characterised by approximately isolated maximum peaks in case of weakly coupled blisks[1]. Reading out the frequencies assigned to the maximum peaks in these FRFs (FIG. 3), blade frequency distributions for each blade mode to be considered can be determined. Since couplings between disk and blades' movement could not be completely eliminated even if a disk clamping device [1], [2] is applied, the blade frequency distribution is related to the particular mean value. It can be shown that the knowledge of a related blade-alone-frequency distribution is sufficient with regard to a determination of increased displacements due to mistuning [3].

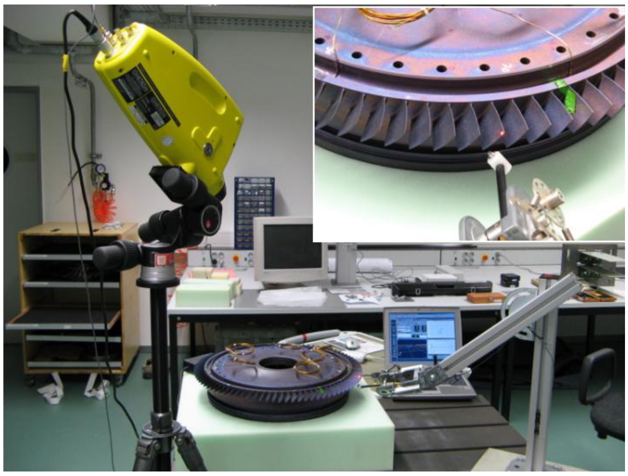

FIG. 2 Experimental set-up for mistuning identification

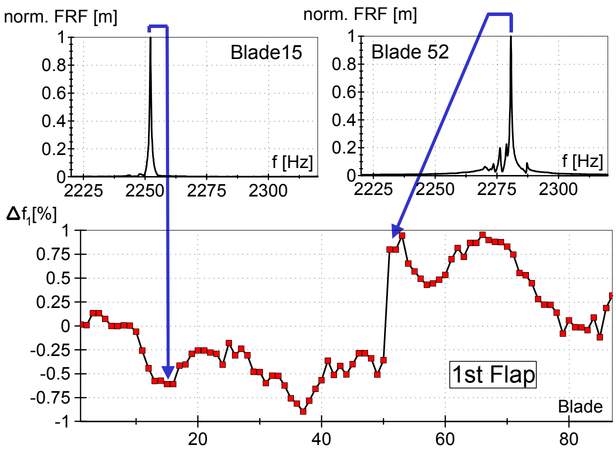

FIG. 3 Procedure of mistuning identification $\Delta f_i = \frac{f_{i,k} - \bar{f}_i}{\bar{f}_i}$

3. NUMERICAL MODEL

In order to carry out forced response analyses of blisks due to aerodynamic excitations usually FE-models are applied in the aero engine industry. In contrast to the common practice a more simple low degree of freedom model called equivalent blisk model (EBM) is introduced in this paper. The EBM (FIG. 4) does not claim to calculate the exact forced response of a real HPC-Blisk in operation, but aims on the clarification of a number of vibration phenomena in principle as given below:

1) Iterative correction of mean level shifts as a result of blade-disk couplings in measured blade frequency distributions so that real blade alone frequency distributions are obtained [4].
2) Forced response analyses with regard to the relevant engine order (EO) excitations to study the differences in the vibration behaviour of tuned and mistuned blisks (e.g. the appearance of localised vibration modes in the mistuned case)
3) Studying the influence of the air flow on the forced response e.g. with regard to possible smoothing effects of localised vibration modes. For this purpose the EBM has to be supplemented with additional aerodynamic elements representing the co-vibrating air mass, air stiffening and aerodynamic damping (see Section 5).

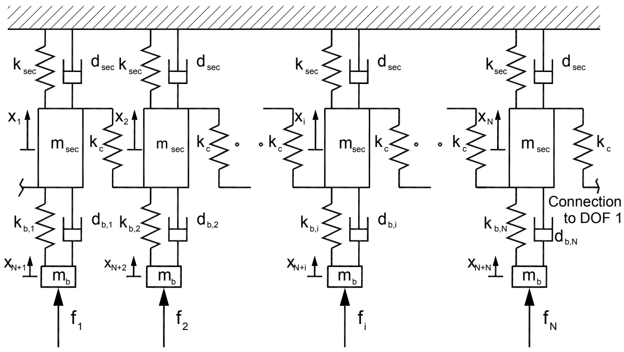

FIG. 4 Equivalent Blisk Model (EBM)

Notations:

N	Number of blades
$k_{b,i}$	Stiffness of ith blade (i. e. according to 1st flap), i = 1..... N
k_d	Disk stiffness
k_{sec}	Sector stiffness
k_c	Coupling stiffness
m_b	Blade mass
m_d	Disk mass
m_{sec}	Sector mass
d_b	Structural blade damping
d_{sec}	Structural sector damping
$f_{b,i}$	Mode-dependent natural blade frequency (i. e. acc. to 1st flap) of ith blade connected to a rigid disk, i = 1.....N
f_i	Exciting force of ith blade

The EBM contains altogether 2N degrees of freedom (DOF) from which x_1 to x_N represent the N sectors of the disk and x_{N+1} to x_{2N} the N blades. The stiffness parameters of the blades are adjusted to measured blade alone frequency distributions and are individually different for each blade and each blade mode considered. Apart from the coupling stiffness k_c, which is iteratively adjusted

[1] In case of weakly coupled blisks the influence of blades which are actually not excited remains small due to a comparatively minor motion of the disk

corresponding to natural frequencies of the disk, all other stiffness and mass parameters can be taken from the design. Information of structural damping parameters is available from blade by blade measurements as well as from results of an experimental modal analysis of the blisk. For more detailed information of the complete EBM-derivation please refer [3] and [4].

4. FORCED RESPONSE ANALYSES

As a first application of the EBM forced response analyses with regard to relevant EOs will be carried out, based on a rotating unit excitation in terms of travelling waves and applied to a stationary test-blisk. From the Campbell-diagram shown in FIG. 5 the necessary EO-information can be taken. For example for the first blade flap mode (1F) resonant excitation can result from an EO 9-excitation.

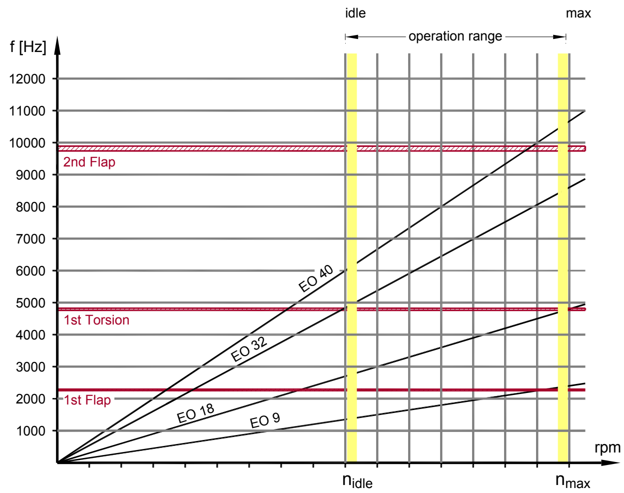

FIG. 5 Campbell diagram of a test-blisk

The excitation $f_i(t)$ of the i^{th} blade (see also [5]) can be written as

(1) $f_i(t) = \cos(\varphi_i + \alpha(t))$, i = 1.......N

in which the angles φ_i define the spatial shape of excitation according to

(2) $$\varphi_i = 2\pi \frac{EO}{N} i$$

and $\alpha(t)$ a time-dependent phase shift describing the rotation:

(3) $$\alpha(t) = 2\pi f_e t$$

f_e denotes the exciting frequency.

The response X(f) or x(t) respectively, can be calculated directly in frequency domain applying the matrix of frequency response functions **H**(f) according to

(4) **X**(f) = **H**(f)**F**(f)

or, what is more time-consuming, with a time step integration method, e. g. the Θ-Wilson method [11].

FIGURES 6 and 7 compare the maximum response of the ideal tuned and the mistuned case without consideration of any aerodynamic damping. It becomes apparent that the tuned vibration mode representing the blade displacements (FIG. 6) is characterised by a pure sine-shape without any localisation which is exemplarily shown for the maximum displacement of the tuned case at 2263.65 Hz. In the mistuned case the sine-shape of the vibration mode gets lost and localisations appear. Although the tuned mode is assigned to the maximum peak in the frequency response it is slightly exceeded by the mistuned mode for Blade 10 at the same frequency .

The situation becomes worse considering Blade 17 at 2256.09 Hz where the mistuned mode reaches its maximum displacement. Induced by the localised mode to be seen in FIG. 7 the maximum displacement of the mistuned case is about 51.3 % higher compared to the tuned case.

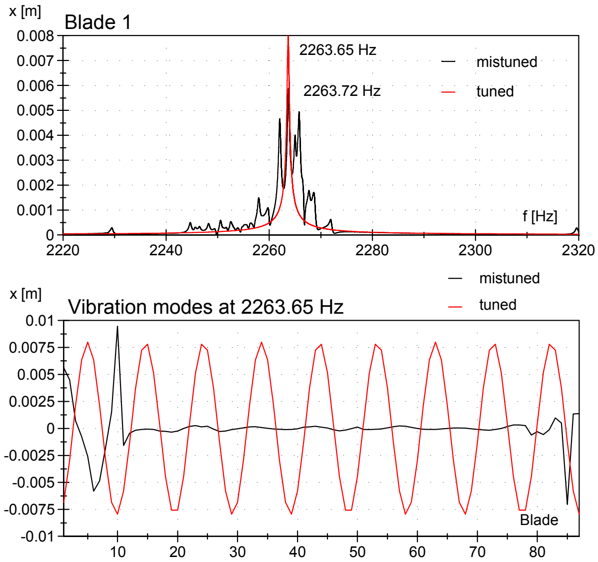

FIG. 6 Maximum forced response (Blade 1, EO 9, 1F)

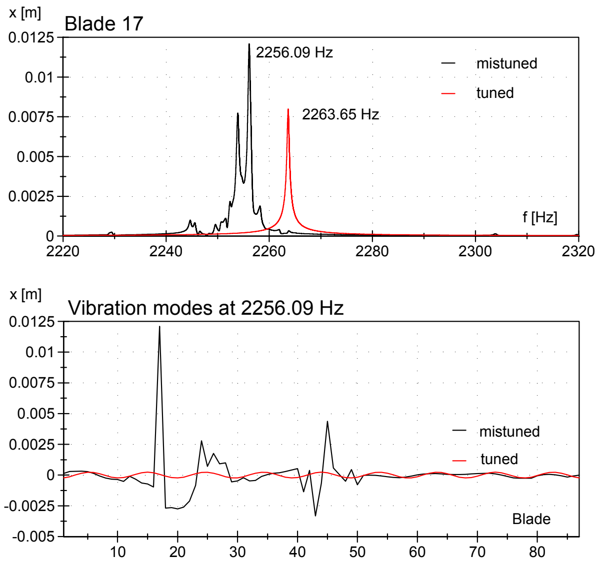

FIG. 7 Maximum forced response (Blade 17, EO 9, 1F)

A suitable measure to assess the degree of localisation is given by

(5) $$\text{Locafac} = \frac{100}{\sqrt{N}-\sqrt{2}}\left(\varsigma-\sqrt{2}\right) \quad [\%]$$

for (M)CSM 1 $\leq$ (M)CSM i $\leq$ (M)CSM$_{max}$

or

(6) $$\text{Locafac} = \frac{100}{\sqrt{N}-1}\left(\varsigma-1\right) \quad [\%] \quad \text{for (M)CSM 0,}$$

with

(7) $$\varsigma = \frac{u_{i,max}}{RMS_{u_i}} \quad ,$$

in which $u_{i,max}$ denotes the maximum displacement of Blade i (i = 1…N), $RMS_{u,i}$ the corresponding root mean square and (M)CSM$_i$ the i^{th} (modified) cyclic symmetry mode. In case of a completely localised vibration mode in which the whole vibration energy in concentrated in one blade Locafac will reach its maximum at 100 %. In contrast, Locafac = 0% is given for tuned blisks. For more detailed descriptions please refer to [6].

In the present case, the mistuning distribution derived from measurement leads to a degree of localisation of 75.66 %, if the absolute maximum of displacement is reached (TAB. 1). As mentioned before the highest amplification of the maximum tuned displacement exceeds 51 %, whereas considering the maximum tuned frequency of 2263.65 Hz the corresponding amplification decreases to 18.6 %.

Thus, the investigations presented before confirm the well known critical influence of mistuning on the forced response [1, 7-10]. However, up to now interacting influences of the flow are neglected. It can be expected that especially additional aerodynamic damping will smooth strongly localised modes and thus reduce negative effects of mistuning. In order to find out more details about these phenomena, an advanced EBM will be introduced in Section 5 which contains additional aerodynamic elements.

f_e [Hz]	ζ [-]	Locafac [%]	max $u_{mistuned}/u_{tuned}$
2256.09	7.401	75.66	1.513 (Blade 17)
2263.65	5.361	49.87	1.186 (Blade 1)

TAB. 1 Effect of mistuning given in FIG. 3 (no aerodynamic damping considered)

5. ADVANCED EBM

Since the interaction between the blisk and the air flow will affect the vibration response in a manifold manner, additional aerodynamic elements (in red colour in FIG. 8) are included in an advanced EBM aiming at a consideration of

- co-vibrating air mass,
- flow-induced stiffness effects between the blades and
- aerodynamic damping.

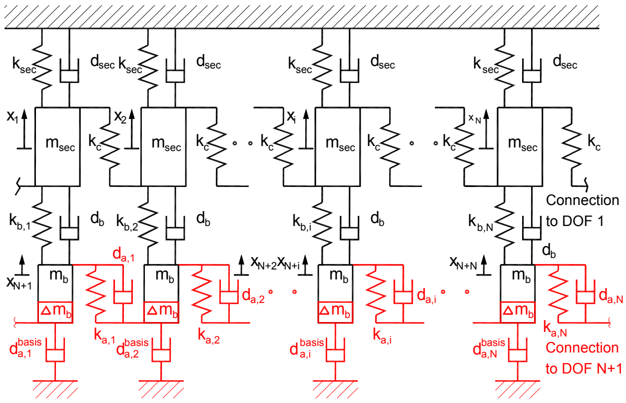

FIG. 8 Advanced EBM

Notations:

Δm_b	co-vibrating air mass
$k_{a,i}$	air stiffness contribution
$d_{a,i}$	aerodynamic inter-blade damping
$d_{a,bas,i}$	aerodynamic basis damping

The co-vibrating air-masses will be added to the blade masses and firstly assumed to be equal and independent from the inter blade phase angle (IBPA). The aerodynamic damping is divided up into a basis part and a part acting between the two adjacent blades, which considers the dependence of the damping force on the IBPA. This means that if adjacent blades vibrate in phase, the damping force of the second part will disappear. The same applies to the supporting force of $k_{a,i}$ between two blades.

Besides the consideration of additional damping, effects of frequency shifts can be calculated with the implementation of the new parameters. What is still open is the question how to choose the aerodynamic quantities in a suitable manner. To get an idea about this, fully coupled FSI-computations will be carried out applying simple blade cascades in which each blade is considered to be rigid but elastically supported. Corresponding models will be introduced in Section 6.

6. FLUID STRUCTURE INTERACTION

In order to get an answer about the FSI close to reality, a partitional coupling between the FE-code ABAQUS and the CFD-code FLUENT via MpCCI is a suitable approach. Based on the geometry of the HPC-Testblisk treated before, a 1,2,3,4 or 5-blade cascade (tuned) depending on the exciting EO is considered. A rigid air foil modelling is applied for this purpose, in which each air foil is elastically supported (FIG. 9). The investigations are based on a 2-dimensional CFD-meanline approach at a blade radial position of 50%, the assumption of a compressible flow (ideal gas) and a focus on the 1^{st} flap mode (1F). In a first approach, maximum take off conditions (MTO) are assumed to define the pressure inlet and outlet conditions. In circumferential direction translational periodicity is applied. Finally, a Spalart Allmaras turbulence model and a hybrid semi-structured CFD-mesh are used as pre-settings.

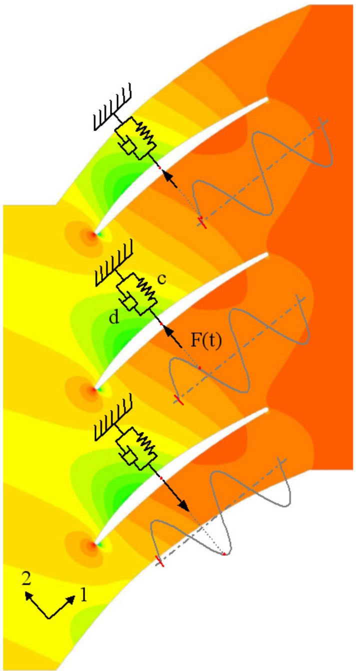

FIG. 9 2-D FSI-Model

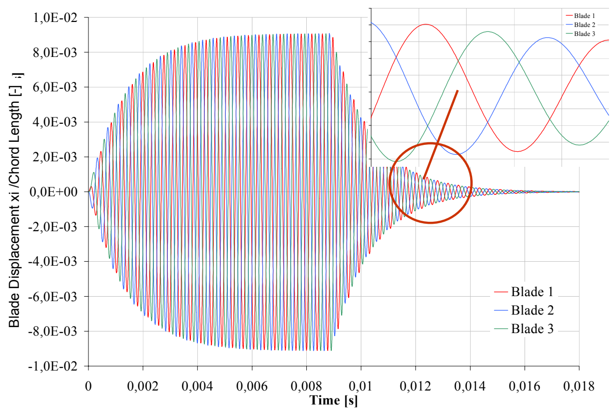

FIG. 10 Blade displacements (3-Blade cascade) due to resonant excitation (switched off after reaching $x_{i,max}$)

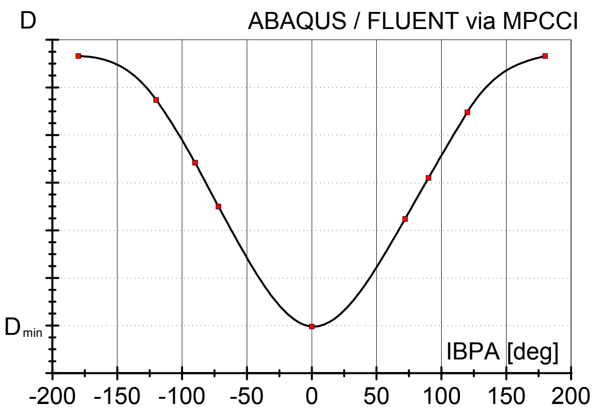

FIG. 11 Dependence of aerodynamic damping on IBPA (MTO)

Aiming at a simulation of a traveling wave EO-excitation, a phase-controlled resonance force excitation on each blade is used. Only 1 translational DOF each is regarded in local 2-direction (FIG. 9). In the case presented in FIG. 10, a 120-degree phase shift simulating a backward traveling wave (BTW) is applied. After reaching a steady state response, the excitation is switched off by which decaying blade displacement curves appear (FIG. 10). From these curves the damping values against the phase-shift (inter blade phase angle, IBPA) can be determined (FIG. 11) calculating the logarithmic decrements. The minimum damping value is obtained for an approximately in-phase excitation (IBPA ≈ 0°) according to an excitation of a CSM 0. With increasing absolute phase angles essentially increased damping values are determined. For further details of the FSI approach please refer to [12].

Based on the forcing F(t) applied (see FIG. 9), the maximum displacement response $x_{i,max}$ due to resonant excitation (FIG. 10) and the damping results shown in FIG. 11, a derivation of the parameters Δm_b, $k_{a,i}$, $d_{a,i}$ and $d_{a,bas,i}$ becomes possible simulating the forced responses of the blade cascades by means of simple low degree of freedom models. A corresponding strategy will be presented in Section 7.

7. DERIVATION OF AERODYNAMIC PARAMETERS

The strategy of derivation is based on the idea to replace the flow in the models of Section 6 with discrete mass, spring and damper elements representing the fluid structure interaction. Thus, for each EO excitation a simple mechanical model is created. Similar to the advanced EBM, the flow influence is completely mapped to the structural level.

Considering an EO 0 excitation, the most simple model – a single degree of freedom model - is generated (FIG. 12).

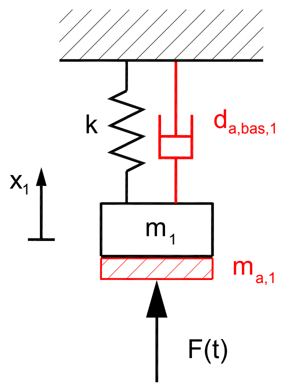

FIG. 12 Mechanical Model for an EO 0 excitation

The equation of motion for the model of FIG. 12 is written as

(8) $(m_1 + m_{a,1})\ddot{x}_1 + d_{a,bas,1}\dot{x} + k_1 x = F(t)$

with the forcing

(9) $F(t) = F_0 \sin(2\pi f \cdot t)$.

It is well-known that the steady state maximum displacement x_{max} is described by the equation

$$(10)\quad x_{max} = \frac{F_0}{k}\frac{1}{\sqrt{(1-\eta^2)^2 + 4D^2\eta^2}}$$

in which the frequency relation η is defined by

$$(11)\quad \eta = \frac{\Omega}{\omega} = \frac{\Omega}{\sqrt{\frac{k}{m_1 + m_{a,1}}}}.$$

Known quantities are the blade mass m_1 and the blade stiffness k from the structural point of view as well as the forcing F_0, x_{max}, the exciting angular frequency Ω and the damping ratio D (FIG. 10) from the FSI-EO 0 computation.

Substituting

$$(12)\quad \alpha = \frac{\Omega^2}{k},$$

$$(13)\quad \gamma = \left[\frac{F_0}{k\,x_{max}}\right]^2 \text{ and}$$

$$(14)\quad m^* = m_1 + m_{a,1}$$

a conditional equation for the unknown parameter m^* and thus $m_{a,1}$ according to

$$(15)\quad m^{*2}\alpha^2 + m^* \cdot 2\alpha(2D^2 - 1) + 1 - \gamma = 0$$

can be derived from (10) to (14). In this way, the co-vibrating air-mass $m_{a,1}$ can be determined to 0.83 % of m_1. The aerodynamic basis damping to be applied in the mechanical model (FIG. 12) is determined by

$$(16)\quad d_{a,bas,1} = 2 \cdot D \cdot m^* \sqrt{\frac{k}{m^*}}$$

and is assumed to remain constant also for higher EO-excitations.

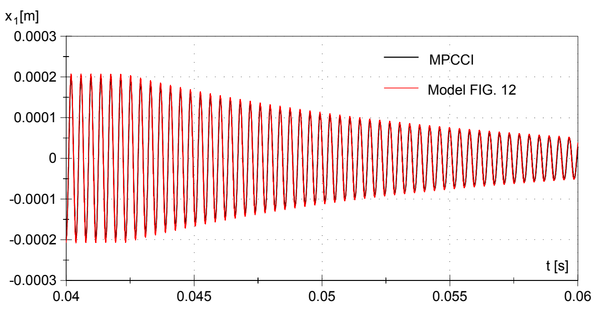

FIG. 13 Decaying displacement curves (MPCCI vs. FIG. 12 – Model)

Comparing the displacements calculated with FSI and those obtained by a Θ-Wilson time step integration method for the 1-DOF-model of FIG. 12 a largely good correlation can be found (FIG. 13). The remaining small deviations result from fact that a steady state response has not been reached within the FSI-approach so that x_{max} has assumed to be about 5 % too low in the derivation process.

If a higher engine order excitation is considered, the IBPA will differ from zero, so that the inter-blade parameters $k_{a,i}$ and $d_{a,i}$ become relevant. This means that corresponding to the FSI-approach multi-DOF-models have to be derived as exemplarily shown for an EO_{max}-excitation in FIG. 14, representing the extreme case of an opposite phase blade motion (IBPA = 180°). Assuming that $m_1 = m_2 = m$, $k_1 = k_2 = k$, $m_{a,1} = m_{a,2} = m_a$, $k_{a,1} = k_{a,2} = k_a$, $d_{a,1} = d_{a,2} = d_a$ und $d_{a,bas,1} = d_{a,bas,2} = d_{a,bas}$, which is the case if a tuned system is considered, the system of differential equations can be written according to Eq. (17).

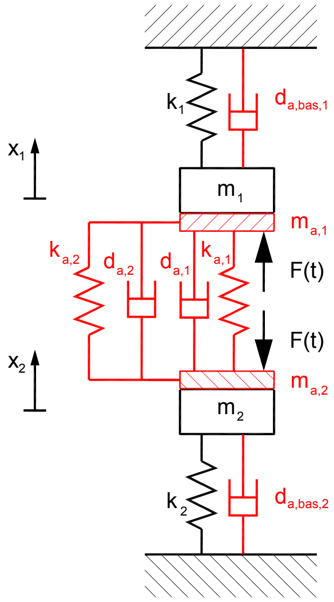

FIG. 14 Mechanical Model for an EO_{max} excitation

$$(17)\quad \begin{bmatrix} m+m_a & 0 \\ 0 & m+m_a \end{bmatrix}\begin{bmatrix} \ddot{x}_1 \\ \ddot{x}_2 \end{bmatrix} + \begin{bmatrix} d_{a,bas}+2d_a & -2d_a \\ -2d_a & d_{a,bas}+2d_a \end{bmatrix}\begin{bmatrix} \dot{x}_1 \\ \dot{x}_2 \end{bmatrix} + \begin{bmatrix} k+2k_a & -2k_a \\ -2k_a & k+2k_a \end{bmatrix}\begin{bmatrix} x_1 \\ x_2 \end{bmatrix} = \begin{bmatrix} F(t) \\ -F(t) \end{bmatrix}$$

The solution for x_i is given by

$$(18)\quad x_i(t) = x_i^s \sin(\Omega t) + x_i^c \cos(\Omega t) \quad \text{or}$$

$$(19)\quad x_i(t) = x_{max}\cos(\Omega t - \varphi_i) \qquad \text{respectively.}$$

Since the maximum displacement x_{max}, the phase angle φ_i and the forcing $F(t) = F_0\sin(\Omega t)$ are known quantities from the FSI-computation and assuming that m_a can be taken from the EO 0-solution, the only unknown quantities in Eq. (17) are d_a and k_a. Introducing the solution x_i in (17) and comparing coefficients according to the sine and the cosine term it becomes clear, that a linear system of equations for the calculation of d_a and k_a can be derived from only one line of (17), here line 1 is chosen:

$$(20)\quad \begin{bmatrix} -4\Omega & 4\tan\varphi_1 \\ 4\Omega\tan\varphi_i & 4 \end{bmatrix}\begin{bmatrix} d_a \\ k_a \end{bmatrix} = \begin{bmatrix} F_0/x_1^c + \Omega^2(m+m_a)\tan\varphi_1 + d_{a,bas}\Omega - k\tan\varphi_1 \\ \Omega^2(m+m_a) - d_{a,bas}\Omega\tan\varphi_1 - k \end{bmatrix}$$

in which x_1^c is

$$(21)\quad x_1^c = x_{max} \cos \varphi_1$$

As already ascertained for the co-vibrating air mass, the air stiffness contribution remains small with 0.55 % of the blade stiffness. This means that it can be expected that the main influence of the air flow results from the aerodynamic damping which is multiple higher than the structural damping part.

In terms of a verification, the parameters identified before are introduced in Eq. (17) and the vibration displacement response is calculated. An excellent correlation with the FSI-solution is obvious (FIG. 15).

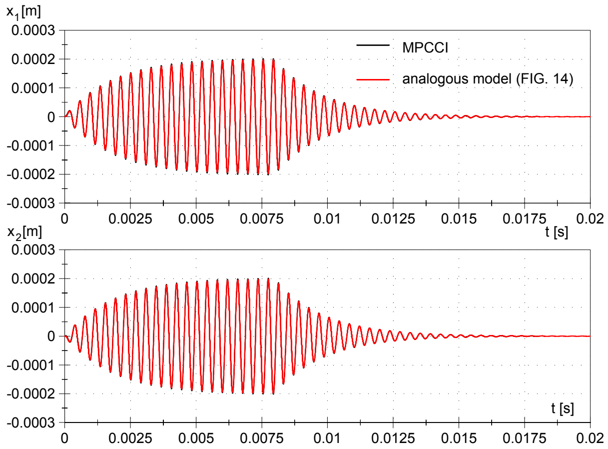

FIG. 15 Decaying displacement curves (MPCCI vs. FIG. 14 – Model)

Analogue to the methodology described before, aerodynamic inter blade parameters are determined for IBPAs of 72° (5 DOF), 90° (4 DOF) and 120° (3 DOF) again considering only one line in the correspondig system of differential equations and deriving a simple system of linear equations as written in Eq. (22):

$$(22)\quad \left[\begin{array}{c|c} \Omega(-2x_1^c + x_2^c + x_N^c) & 2x_1^s - x_2^s - x_N^s \\ \hline \Omega(x_1^s - x_2^s - x_N^s) & 2x_1^c - x_2^c - x_N^c \end{array}\right] \begin{bmatrix} d_a \\ k_a \end{bmatrix} = \begin{bmatrix} F_0 + \Omega^2(m+m_a)x_1^s + d_{a,bas}\Omega x_1^c - kx_1^s \\ \Omega^2(m+m_a)x_1^c - d_{a,bas}\Omega x_1^s - kx_1^c \end{bmatrix}$$

with

$$(23)\quad x_i^s = x_{max} \sin \varphi_i$$

Apart from an IBPA of 0° the right hand side of Eq. (20) remains the same. On the left hand side only x_N^s and x_N^c change in dependence on the number of DOF. Plotting the d_a –values versus IBPA as shown in FIG. 16 an approximately linear dependence can be found. It should be mentioned that this does not mean that the damping force also changes in a linear manner. Furthermore the separate part $d_{a,bas}$ completes the damping contribution of the FSI. Compared to d_a the correlation between k_a and IBPA is not that clear, but remains small, so that a constant mean value is applied for further investigations.

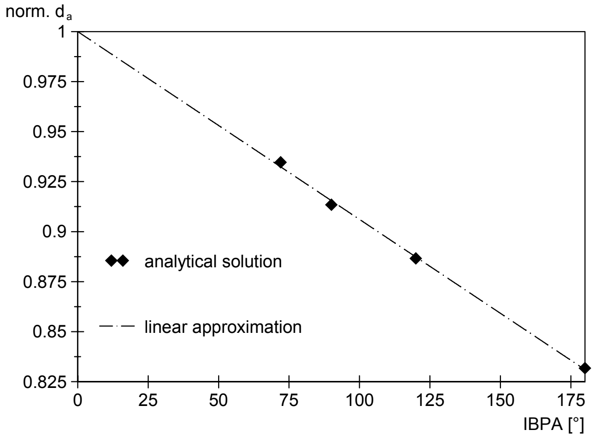

FIG. 16 Inter blade damping vs IBPA

8. FORCED RESPONSE CONSIDERING THE INFLUENCE OF AIR FLOW

Including the aerodynamic parameters identified in Section 7 into the advanced EBM, a forced response analysis similiar to the approch presented in Section 4 is carried out. Indeed, due to the dependence of d_a and k_a from IBPA, an iterative approach becomes necessary. As stated before, k_a will be kept constant due to its comparatively small influence. However, d_a will be individually adopted corresponding to the phase difference between two adjacent blades until the maximum blade displacements do not change any more. This procedure has to be carried out for each frequency excited. Due to the individually different allocation of d_a for each blade an additional index i ($d_{a,i}$) as shown in FIG. 8 becomes necessary. Results of two different sets of parameters are presented in this paper (EO 9, 1F):

1) In order to study the influence of the important inter blade damping d_a all other aerodynamic parameters are assumed to be zero (FIGS. 17 and 18).
2) All aerodynamic influences are considered as calculated in Section 7 (FIGS. 19 and 20).

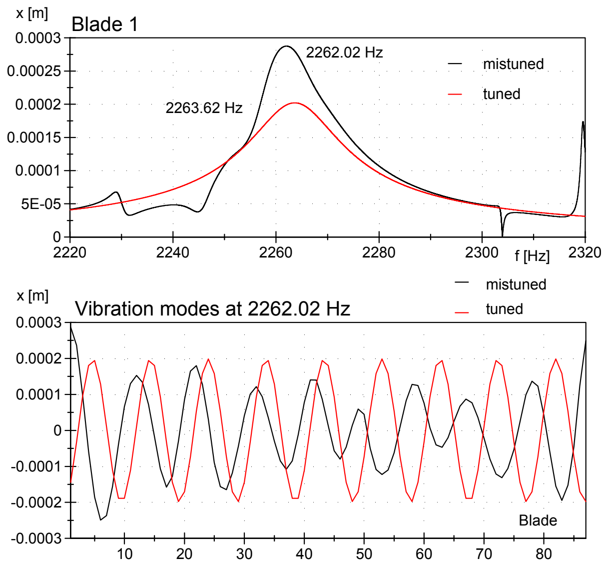

FIG. 17 Maximum forced response (Blade 1, EO 9, 1F, $d_{a,i}$ considered)

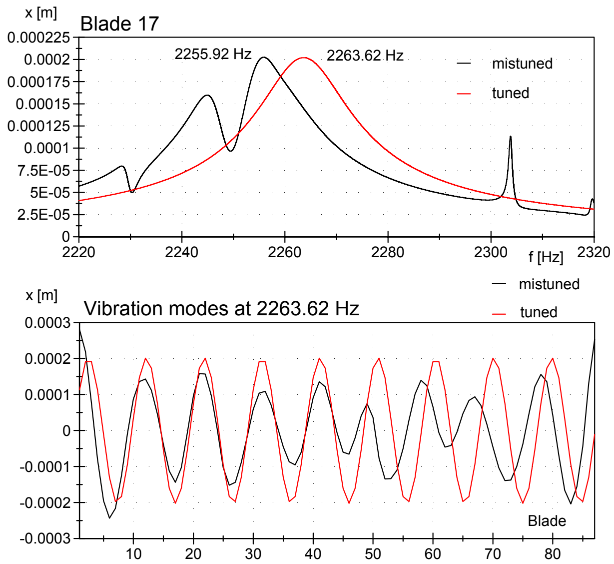

FIG. 18 Maximum forced response (Blade 17, EO 9, 1F, $d_{a,i}$ considered)

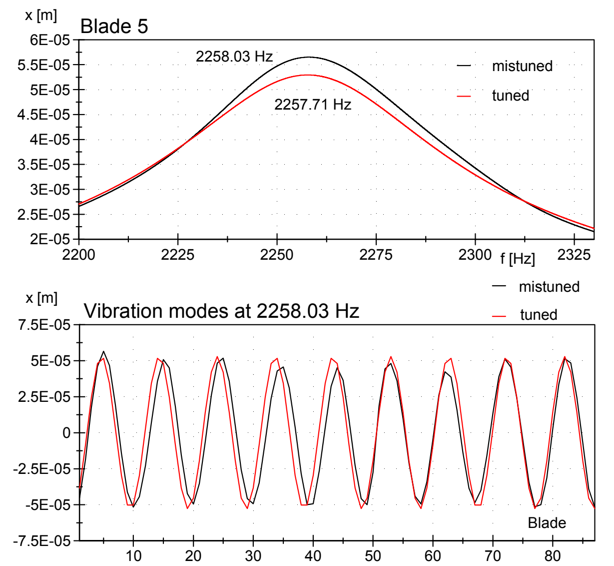

FIG. 19 Maximum forced response (Blade 5, EO 9, 1F, all aerodynamic influences considered)

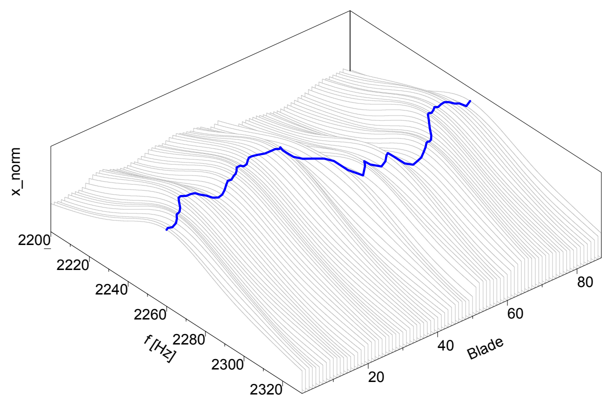

FIG. 20 Forced response (EO 9, 1F, all aerodynamic influences considered)

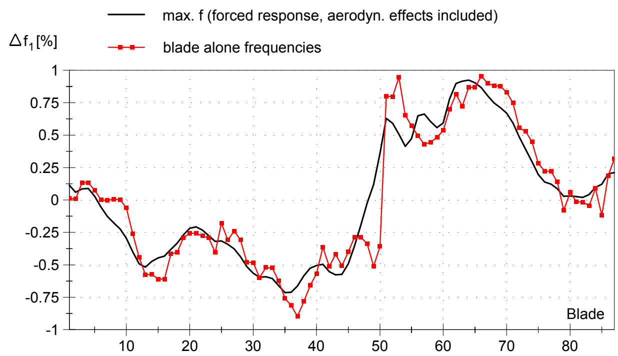

FIG. 21 Frequency of forced response maximum peaks (EO 9) vs blade alone frequency distribution (1F)

EO 9, 1F	no aero-effects	only $d_{a,i}$ considerd	all effects
f_{peak} [Hz]	Locafac (of modes assigned to the highest displacements as shown in FIG. 18)		
2256.09	75.66 %	9,63 % *(-87,3 %)*	1,93 % *(-97,4 %)*
2258.03	49.63 %	9.17 % *(-81,5 %)*	1,96 % *(-96,1 %)*
2262.02	25,66 %	14,03 % *(-45,3 %)*	1,92 % *(-92,5 %)*
max $u_{mistuned}/u_{tuned}$	1.513	1.423	1.068

TAB. 2 Degree of localisation and maximum response amplification in dependence of aerodynamic influences

Regarding the results obtained within the study of the inter blade's damping influence, a general smoothing of the frequency response as well as the vibration modes (FIGS. 17 and 18) compared to the case in which aerodynamic influences are neglected (FIGS. 6 and 7) is obvious. This means that the distinct splitting of individual frequency peaks gets largely lost and mistuned vibration modes tend to take the shape of tuned modes. Nevertheless, although strong localisations disappear, the maximum amplification still reaches a factor of more than 1.42 (TAB. 2), which is not extremely lower compared to the situation without consideration of aerodynamic influences. However, with respect to the degree of localisation a decrease of more than 45 % for the frequency assigned (2262.02 Hz, TAB. 2) is determined. From this it can be reasoned that the worst blade strain level is also decreased in higher degree than the reduction of displacements. Furthermore, It should be mentioned that the absolute displacement maximum is now reached at Blade 1 instead of Blade 17.

If all aerodynamic effects are considered, the smoothing of mistuned vibration modes and frequency responses reaches a degree that the tuned and the mistuned situation seems to merge (FIG. 19). The maximum amplification of displacements now remains below 7 % and the degree of localisation is reduced to less than 2 % coming from approximately 50 % if a frequency of 2258.03 Hz is considered where the maximum displacement appears. Despite of the smoothing effect the general shape of the blade mistuning is still reflected in the distribution of maximum peaks as shown by the boldly plotted curve in FIGS. 20 and the comparison presented in FIG. 21. This means that the effect of mistuning is still verifiable but essentially reduced in present study.

It should be kept in mind that the results presented before are focussed on an MTO-excitation of the first blade flap mode in a rear HPC-Rotor, in which comparatively high compression ratios are achieved. Thus, the present investigation represents an extreme case and it can be expected that the influence of the FSI will be alleviated for higher blade modes (e. g. 2F, 1st torsion, etc.) and HPC-rotors located more up-stream.

9. CONCLUSIONS

Applying an advanced equivalent blisk model which is suited to consider the FSI in a simplified manner, a distinct influence of the air flow on the blisk vibration behaviour could be proved in principle. The investigations are exemplarily carried out for a rear HPC-test-blisk stage with a focus on the first blade flap mode and MTO-conditions, which altogether represents an extreme case with regard to the FSI. Apart from a general reduction of displacement amplitudes caused by the aerodynamic damping, a number of phenomena could be highlighted:

1) The co-vibrating air-mass as well as air stiffening effects between adjacent blades play a minor role
2) A smoothing of the mistuned frequency response and mistuned vibration modes caused by the fixed and the blade phase-dependent aerodynamic damping parts can be noticed
3) Strong localisations disappear. The amplification of the tuned response due to mistuning is reduced, but not eliminated.
4) The blade showing the highest displacements changes due to aerodynamic influences
5) Even if all aerodynamic influences are considered, the distribution of maximum peaks largely corresponds to the mistuning distribution obtained in blade by blade measurements

Despite of 4), the item 5) justifies the current practice of an optimum selection of blades to be applied with strain gauges for rig-tests.

What is still open is an extension of the investigations presented before to higher blade modes (e. g. 1T, 2F, 2T etc.) as well as to HPC-front stages. It is expected that the flow-induced effects on the vibration behaviour will be alleviated especially with regard to the high aerodynamic damping ratios.

Acknowledgments

The work presented before has been supported by the Rolls-Royce Deutschland company. The authors thank for this commitment. The investigations are part of the research project DeSK Blisk Validation (FKZ: 80121978) which is funded by the Federal State of Brandenburg and the European program for regional development (efreinfo@mw.brandenburg.de).

10. REFERENCES

[1] Beirow, B., Kühhorn, A., Golze, M., Klauke, Th., Parchem, R.: Experimental and Numerical Investigations of High Pressure Compressor Blades Vibration Behaviour Considering Mistuning; Proc. of 10th Int. NAFEMS World Congress, 2005, Malta.
[2] Beirow, B., Kühhorn, A., Klauke, Th.: Localisation Phenomenon at Blade Integrated Disks (Blisks), Schwingungen in Antrieben, Fulda, VDI-Berichte Nr. 1968, 2006 (in German).
[3] Beirow, B., Kühhorn, A., Schrape, S.: Blisk Vibration Phenomena in Consideration of Fluid Structure Interaction. Proc. of 11th Int. NAFEMS World Congress, 2007, Vancouver.
[4] Kühhorn, A., Beirow, B.: An Equivalent Model for Forced Response Sensitivity Analyzes. Journal of Turbomachinery (TURBO-07-1020, paper under review).
[5] Rivas-Guerra, A. J., Mignolet, M. P.: Local/Global Effects of Mistuning on the Forced Response of Bladed Disks. Journal of Engineering for Gas Turbines and Power, Vol. 126, pp.131-141, 2004.
[6] Kühhorn, A., Beirow, B., Parchem, R., Klauke, T.: Schaufelschwingungen bei realen Verdichterrädern. Proc. of DGLR-Congress, Braunschweig, 2006 (in German).
[7] Jugde, J., Pierre, C., Mehmed, O., 2001, "Experimental Investigation of Mode Localisation and Forced response Amplitude Magnification for a Mistuned Bladed Disk", ASME J. of Engineering for Gas Turbines and Power, 123, pp. 940-950.
[8] Petrov, E. P., Ewins, D. J., 2003, "Analysis of the Worst Mistuning Patterns in Bladed Disk Assemblies", ASME Journal of Turbomachinery, 125, pp. 623-631.
[9] Kenyon, J. A., Griffin, J. H., Feiner, D. M, 2003, „Maximum Bladed Disk Forced Response From Distortion of a Structural Mode", ASME Journal of Turbomachinery, 125, pp 352-363.
[10] Whitehead, D. S, 1998, The Maximum Factor by Which Forced Vibration of Blades Can Increase Due to Mistuning, ASME Journal of Engineering for Gas Turbines and Power, 120, pp. 115-119.
[11] Wilson, E. L., Farhoomand, I., Bathe, K.J., 1973, Nonlinear Dynamic Analysis of Complex Structures. Journal of Earthquake Engineering and Structural Dynamics, 1, pp.241-252.
[12] Schrape, S., Kühhorn, A.: FSI of a Simplified Aero Engine Compressor Cascade Configuration. Proc. of GAMM Annual Meeting, March 27-31, Berlin, 2006.
[13] Ewins, D. J., 1976, Vibration Modes of Mistuned Bladed Disks, Journal of Engineering for Gas Turbines and Power, 120, pp. 115-119.
[14] Fraunhofer Institute for Algorithms and Scientific Computing SCAI, MpCCI 3.0.6, MpCCI Documentation, 2007. http://www.mpcci.de/